Hemangiopericytoma in a cat: a case report

A. Blutke[1], J. Knebel[2], A. Brühschwein[2], W. Breuer[3], W. Hermanns[1]

[1]Institute of Veterinary Pathology at the Centre for Clinical Veterinary Medicine, Ludwig-Maximilians-Universitaet München, Munich, Germany
[2]Clinic of Small Animal Surgery and Reproduction at the Centre for Clinical Veterinary Medicine, Ludwig-Maximilians-Universitaet München, Munich, Germany
[3]Bayerisches Landesamt für Gesundheit und Lebensmittelsicherheit, Oberschleißheim, Germany

ABSTRACT: In dogs and men, hemangiopericytoma is a well-recognised neoplasm, thought to originate from vascular pericytes. In cats, however, hemangiopericytoma is an extremely rare finding. The present report describes the pathological features of a 7-cm-diameter, dense, white, multilobulated tumour-like growth on the thigh of a ten-year-old Persian cat. Histologically, the mass consisted of polygonal neoplastic cells, concentrically arranged around thin-walled endothelium-lined blood vessels occasionally forming typical staghorn-configurations. In reticulin-stained sections, a dense meshwork of argyrophilic collagen fibres was evident, surrounding the central vessels and separating individual tumour cells. Within the tumour tissue, there were areas of extensive necrosis and degeneration. In the periphery, the tumour displayed a moderate infiltrative growth into the adjacent musculature. Immunohistochemical analysis revealed strong diffuse cytoplasmatic immunoreactivity for vimentin, a focal immunoreactivity for S-100, and a weak interstitial staining for laminin, whereas neoplastic cells stained negative for cytokeratin, desmin, actin, calponin, von Willebrand factor, glial fibrillary acidic protein, neuron specific enolase, CD79a, MAC387, lysozyme and MHCII. Ultrastructurally, the neoplastic cells contained few intracytoplasmatic filaments, and were surrounded by interlacing bundles of intercellular long-spacing collagen fibres. Occasionally, desmosome-like intermediate junctions were observed between neighbouring tumour cells. On the basis of histomorphology, ultrastructure and immunohistochemical reactivity, the neoplasm was diagnosed as a hemangiopericytoma, representing the second reported case of this rare tumour entity in a cat.

Keywords: electron microscopy; immunohistochemistry; pericyte; perivascular; tumor

In humans and dogs, hemangiopericytoma (HEP) is a mesenchymal neoplasm thought to originate from capillary subendothelial pericytes (Enzinger and Weiss 1995; Goldschmidt and Hendrick 2002; Gross et al. 2005). In humans, HEP is considered a malignant neoplasm with a reported incidence of approximately 2.5% of all soft tissue sarcomas. HEPs are most frequently found in the lower extremities, especially in the thigh. They usually present as solitary, well cirumscribed, lobulated and pseudocapsulated masses of gray-white to red-brown color, and measure from one to more than 20 cm in diameter. The metastatic potential of human HEP is reported to be highly variable, with metastatic rates ranging from 11 to more than 50 per cent (Enzinger and Weiss 1995). In dogs, HEP has been reported as a frequent neoplasm, accounting for 7% of canine skin tumours (Gross et al. 2005). Canine (C) HEPs are most often found at the extremities of middle-aged to old dogs and usually appear as subcutaneous, lobulated, firm, white to grey coloured tumours, occasionally reaching considerable dimensions (Mulligan 1955; Goldschmidt and Hendrick 2002; Gross et al. 2005). They frequently display a locally infiltrative growth and tend towards recurrence after surgical excision; however, metastatic spread is uncommon (Goldschmidt and Hendrick 2002; Gross et al. 2005). The histopathological features of CHEPs are quite different from human HEPs (Goldschmidt and Hendrick 2002). Human HEPs usually consist of tightly packed cells with round to oval nuclei and moderate amounts of

cytoplasm, concentrically arranged around ramifying, thin-walled, endothelium-lined vascular channels, occasionally forming a typical "antler-like" or staghorn configuration. The tumour cells are mostly enmeshed by reticulin and collagen fibres and separated from the constituent vessels by a continous basal lamina, which can be outlined using PAS or reticulin staining (Enzinger and Weiss 1995). The number of mitotic figures per high power field is variable, which has been used as a prognostic criterion to predict the tumour's biological behaviour (Enzinger and Weiss 1995; Handharyani et al. 1999). The canine HEP, however, is characterized by the presence of perivascular whorls, interlacing bundles and sheets of mostly spindle-shaped to fusiform cells with poorly defined cytoplasm, elongated pale nuclei with small central nucleoli, and an usually low mitotic activity (Goldschmidt and Hendrick 2002; Gross et al. 2005). CHEPs with large numbers of whorls around central vessels appear in a typical 'fingerprint' pattern, whereas tumours with abundant stromal mucin often exhibit a more myxoid growth pattern. Areas of necrosis, fibrosis and haemorrhage are frequently observed within the tumour tissue (Gross et al. 2005). Unlike most other mesenchymal neoplasms, both human and canine HEPs lack characteristic immunohistochemical features (Enzinger and Weiss 1995; Goldschmidt and Hendrick 2002; Gross et al. 2005). HEPs are solely found to consistently stain positive for vimentin. The immunoreactivity of HEPs for cytoskeletal and contractile proteins (desmin, alpha smooth muscle actin, calponin, panactin), neural markers (S-100 protein, glial fibrillary acidic protein, neuron specific enolase), cell surface proteins (CD34 and CMG-3G5), or markers of extracellular matrix proteins (laminin) however, has been reported to be highly variable and discordant (Enzinger and Weiss 1995; Handharyani et al. 1999; Sawamoto et al. 1999; Goldschmidt and Hendrick 2002; Mazzei et al. 2002; Chijiwa et al. 2004; Gross et al. 2005; Avallone et al. 2007). Ultrastructurally, the neoplastic cells in (C) HEPs are commonly separated by variable amounts of intervening extracellular collagen fibres and form complex interdigitating processes of inconsistent length with the formation of variable numbers of intermediate desmosome-like intercellular junctions. On the subcellular level, some intracytoplasmatic actin-like microfilaments, micropinocytotic vesicles and dilated rough endoplasmatic reticulum may be present (Henderson et al. 1986; Xu 1986). Histopathological diagnosis of HEP is often difficult, since, although HEPs may exhibit some characteristic histological, immunohistochemical and ultrastructural features, these are not specific for HEP, and can also be found in a large number of other soft tissue neoplasms (Henderson et al. 1986; Enzinger and Weiss 1995; Gross et al. 2005; Avallone et al. 2007). Recent studies actually indicate that HEPs have been overdiagnosed in both humans and dogs, as the term "hemangiopericytoma" was often used to denote a histologic perivascular whorling pattern of tumour cells, rather than a specific neoplasm of pericytes (Gross et al. 2005; Avallone et al. 2007). A diagnostic differentiation of HEP from other neoplasms with a similar morphological appearance however, has crucial clinical significance, since some of these tumour entities exhibit substantial differences in their biological behaviour and prognostic validation. In human medicine, most of the pericytic/perivascular tumours previously designated as hemangiopericytomas have therefore now been reclassified as other types of tumours, and, according to the current World Health Organization (WHO) classification of tumours, only a small group of neoplasms designated as HEPs remains (Fletcher et al. 2002). Although evidence exists that also the canine HEP still embodies a broad spectrum of diverse neoplastic entities of, e.g., perivascular wall tumours with potentially different malignancies (Avallone et al. 2007), a further specific classification of these tumour entities has yet not been implemented in veterinary medicine (Hendrick et al. 1998). Notably, records of HEPs in animals have almost completely been restricted to dogs. In cats, the appearance of a HEP has merely been documented in a single case report by Baldi and Spugnini (2006), who provided a comprehensive description of the morphological characteristics of a tumour resembling the human HEP rather than the canine counterpart. The present report now describes the pathological features of a second case of a hemangiopericytoma in a cat.

Case description

A ten-year-old, neutered male Persian cat was presented to the Clinic for examination of a dense tumour-like growth on the left thigh, which had developed over a period of several months. The excrescence had a size of approximately 10 × 7 × 6 cm, with poorly delimitable borders, and displayed an

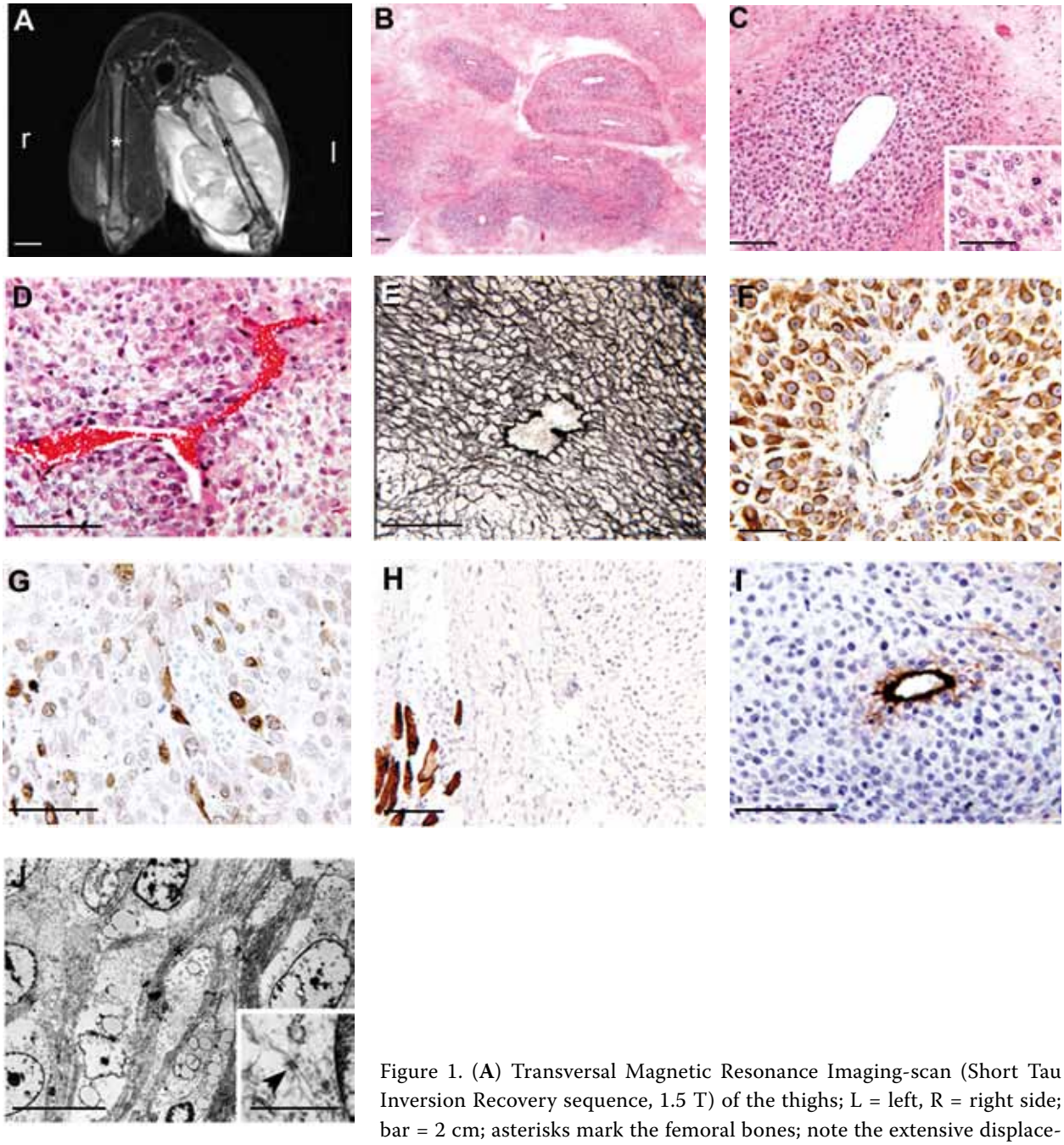

Figure 1. (**A**) Transversal Magnetic Resonance Imaging-scan (Short Tau Inversion Recovery sequence, 1.5 T) of the thighs; L = left, R = right side; bar = 2 cm; asterisks mark the femoral bones; note the extensive displacement of the leg musculature by the tumour. (**B**) Characteristic perivascular growth pattern of tumour cells with extended areas of degeneration and necrosis; paraffin section; H&E staining; bar = 100 µm. (**C**) Central vessels are lined by a flat endothelium and surrounded by polygonal tumour cells with large ovoid nuclei and distinct nucleoli; glycolmethacrylate and methylmethacrylate section (GMA/MMA); H&E staining; bar = 100 µm; inset: detail enlargement of neoplastic cells; mitotic figure (arrowhead); GMA/MMA section; H&E staining; bar= 50 µm. (**D**) Branching of vessels in a typical staghorn configuration. (**E**) A dense meshwork of reticulin fibres surrounds tumour cells and vessels; paraffin section; reticulin staining; bar = 100 µm. (**F-I**) Immunohistology. (**F**) Tumour cells and endothelium stain positive for vimentin; bar = 100 µm. (**G**) Focal positivity of tumour cells for S-100; bar = 50 µm. (**H**) Tumour cells stain negative for desmin; adjacent muscular fibres stain desmin-positive; bar = 100 µm. (**I**) Endothelium of central vessels stains positive for von Willebrand factor; bar = 100 µm. (**J**) Transmission electron microscopy. Tumour cells are separated by bundles of intercellular long-spacing collagen fibres (asterisk); bar = 10 µm; inset: desmosome-like cell-to-cell contacts (arrow) between neighbouring tumour cells are occasionally present; bar = 1 µm

extensive invasiveness into the leg musculature, as evidenced by Magnetic Resonance Imaging[a] (Figure 1A). Based on these findings, the presumptive diagnosis of a malignant neoplasm was made. Due to the poor prognosis, the patient's owner did not agree to any further examinations or surgical intervention, and the cat was therefore euthanised. A comprehensive necropsy of the animal carcass could not be performed, since the owner wished to have the cat incinerated in a pet crematory. For scientific interest, a ~2 cm^3 specimen was excised from the periphery of the white, multilobulated tumour and fixed in 10% formalin for histopathological evaluation. Sections of paraffin-embedded samples and of glycolmethacrylate/methylmethacrylate-embedded samples (Hermanns et al. 1981) were routinely prepared and stained with haematoxylin and eosin (HE) and reticulin preparation. Immunohistochemistry was performed using antibodies specific for vimentin[b], cytokeratin[c], CD79a[d], MHCII[e], von Willebrand factor[f], actin[g], calponin[h], desmin[i], S-100 protein[j], GFAP[k], NSE[l], MAC387[m], lysozyme[n] and laminin[o]. For detection of S-100, von Willebrand factor, CD79a, MHCII, NSE and GFAP, the standard avidin-biotin peroxidase complex method[p,q] was employed. Immunostaining of cytokeratin, vimentin, desmin, actin, calponin, MAC387 and lysozyme was performed using horseradish peroxidase-coupled secondary antibodies[r,s]. Diaminobenzidine was used as the final chromogen and hemalaun as nuclear counterstain. Positive control slides consisted of cat mesenterium including blood vessels and peripheral nerves (actin, calponin, desmin, von Willebrand factor, S-100), skin (cytokeratin), lymph node (CD79a, MHCII, MAC387, lysozyme), skeletal musculature (desmin), spinal cord (S-100, NSE, GFAP), and kidney (laminin). For a negative control, slides containing the tumour and the tissues used for positive control were stained with buffer instead of the primary antibody. Transmission electron microscopy[t] was performed on ultrathin sections of Epon-embedded samples, according to standard procedures. Histologically, the tumour was composed of cuff-like configurations of polygonal cells, concentrically arranged around thin-walled endothelium-lined blood vessels (Figure 1B, C). The central vessels occasionally formed typical staghorn-configurations (Figure 1D). In the periphery, the tumor displayed a moderate infiltrative growth into the adjacent musculature. Between individual tumor-cell-sheathed vessles, there were areas of extensive necrosis and degeneration, attended by the accumulation of mucoid interstitial material (Figure 1A). The neoplastic cells displayed an eosinophilic cytoplasm and large ovoid nuclei with distinct nucleoli. Mitotic figures were frequently observed (Figure 1C), and the mitotic rate was determined to account for 5.6 ± 1.5 per high power field. In reticulin stained sections, a dense meshwork of argyrophilic collagen fibres was evident, surrounding the central vessels and separating individual tumour cells (Figure 1E). Immunohistochemically, the neoplastic cells stained positive for vimentin (Figure 1F), focally positive for S-100 (Figure 1G) and negative for cytokeratin, desmin (Figure 1H),

[a]Symphony Magnetom, Siemens, Germany, [b]Monoclonal Mouse Anti-Vimentin, Clone V9, 1 : 300, Code No. M0725, DakoCytomation, Denmark, [c]Monoclonal Mouse Anti-Human Cytokeratin, Clones AE1/AE3, 1 : 50, Code No. M3515, DakoCytomation, Denmark, [d]Monoclonal Mouse Anti-Human CD79αcy, Clone HM57, 1 : 20, Code No. M7051, DakoCytomation, Denmark, [e]Monoclonal Mouse Anti-Human HLA-DR Antigen, Alpha Chain (MHCII), Clone TAL.1B5, 1 : 200, Code No. M0746, DakoCytomation, Denmark, [f]Polyclonal Rabbit Anti-Human von Willebrand Factor, 1 : 200, Code No. A0082, DakoCytomation, Denmark, [g]Monoclonal Mouse Anti-Human Muscle Actin, Clone HHF35, 1 : 50, Code No. 0635, DakoCytomation, Denmark, [h]Monoclonal Mouse Anti-Calponin, 1 : 1500, Code No. C2687, Sigma-Aldrich, Germany, [i]Monoclonal Mouse Anti-Human Desmin, Clone D33, 1 : 50, Code No. M0760, DakoCytomation, Denmark, [j]Polyclonal Rabbit Anti-S-100, 1 : 400, Code No. 20311, DakoCytomation, Denmark, [k]Polyclonal Rabbit Anti-Glial Fibrillary Acidic Protein, 1 : 500, Code No. 20334, DakoCytomation, Denmark, [l]Neuron specific enolase (NSE) rabbit pAb, 1 :500, Cat. No. NA1247, ENZO Lifesciences, Switzerland, [m]Monoclonal Mouse Anti-Human Myeloid/Histiocyte Antigen, Clone MAC387, 1 : 300, Code No. M0747, DakoCytomation, Denmark, [n]Polyclonal Rabbit Anti-Human Lysozyme, EL3.2.1.17, 1 : 50, Code No. A0099, DakoCytomation, Denmark, [o]Rabbit Anti-Laminin, 1 : 50, Code No. Z0097, DakoCytomation, Denmark, [p]Biotynilated Goat Anti-Rabbit Immunoglobulins, 1 : 200, Code No. E0432, DakoCytomation, Denmark, [q]Polyclonal Goat Anti-Mouse Immunoglobulins/Biotynilated, 1 : 200, Code No. E0433, DakoCytomation, Denmark, [r]Peroxidase Conjugated Rabbit Anti-Mouse Immunoglobulins, 1 : 100, Code No. P0161, DakoCytomation, Denmark, [s]Polyclonal Swine Anti-Rabbit Immunoglobulins/HRP, 1 : 100, Code No. P0217, DakoCytomation, Denmark, [t]Zeiss EM 10 electron microscope, Zeiss, Germany

actin, calponin, GFAP, NSE, CD79a, MAC387, lysozyme and MHCII. Positive immunoreactivity for von Willebrand factor within the tumour was restricted to the endothelium of the central vessels (Figure 1F). The subendothelial vascular basement membranes stained positive for laminin, whereas the intercellular argyrophilic fibres between individual tumour cells only displayed a weak immunoreactivity against this basement membrane marker (data not shown). Ultrastructurally, the tumour cells were surrounded by interlacing bundles of long-spacing collagen fibres (Figure 1J), corresponding to the reticulin staining pattern in paraffin sections. The central blood vessels were differentiated from neoplastic cells by a poorly developed, but continuous basement membrane. Desmosome-like intermediate junctions between neighbouring tumour cells were occasionally observed (Figure 1J). The neoplastic cells contained some intracytoplasmic filaments, mitochondria, some free ribosomes, lysosomal vesicles and partially dilated rough endoplasmatic reticulum. Histopathologically, the strict perivascular growth pattern and typical vascular staghorn configuration of the neoplasm, the uniform cellularity, and the dense reticulin meshwork surrounding the individual tumour cells suggested that the tumour was a HEP (Enzinger and Weiss 1995; Gross et al. 2005). This diagnosis was supported by the immunohistological findings, consistent with a mesenchymal neoplasm without evidence of histiocytic, lymphoid or endothelial origin, or smooth-muscular differentiation. Also, the ultrastructural features of the tumour cells were in conformity with those of HEP (Henderson et al. 1986; Xu 1986). Moreover, the morphological and immunohistochemical features of the neoplasm were almost identical to that of a feline HEP described by Baldi and Spugnini (2006).

DISCUSSION AND CONCLUSIONS

Since HEPs lack specific or unique histopathological properties, to distinguish HEP from other neoplasms with prominent whirling or perivascular growth patterns may cause considerable difficulties. In humans and dogs, essential differential diagnoses for HEP include peripheral nerve sheath tumour, fibrosarcoma, histiocytic sarcoma, vascular neoplasms, perivascular wall tumours and glomus tumours (Henderson et al. 1986; Enzinger and Weiss 1995; Sawamoto et al. 1999; Mazzei et al. 2002; Chijiwa et al. 2004; Gross et al. 2005; Baldi and Spugnini 2006; Avallone et al. 2007). In particular, the differentiation of HEP from peripheral nerve sheath tumours (PNST) can be difficult, since neoplastic cells in PNSTs may display similar morphological features as in HEPs, and are often arranged in whorls. However, the whorls present in PNSTs are less prominent and not strictly centred on vascular structures (Gross et al. 2005). In contrast to HEPs, PNSTs frequently have interlacing wavy bundles of tumour cells (Antony type A pattern), fusiform and serpentine nuclei and variable palisading of neoplastic cells. The Schwannian differentiation in PNSTs is supported by a regularly positive immunoreactivity against S-100, GFAP and NSE (Goldschmidt and Hendrick 2002; Chijiwa et al. 2004; Gross et al. 2005; Schulman et al. 2009). In the present case, the uniform cellular and perivascular pattern of the tumour, and the absence of immunoreactivity against GFAP and NSE helped to rule out a diagnosis of PNST. Fibrosarcomas display similar cellular characteristics as CHAPs, and may also exhibit whirling of tumour cells. However, these perithelioma-like structures are arranged around collagenous centres, whereas concentric perivascular whorls are unusual (Gross et al. 2005). Histiocytic sarcomas may also occasionally display an irregularly whorled, storiform growth pattern, but are devoid of concentric perivascular whorls (Gross et al. 2005). Additionally to different morphological features, the lack of tumour cell-immunoreactivity against lysozyme, MHC class II and MAC387, contributed to exclude the differential diagnosis of a neoplasm of histiocytic/dentritic cells in the present case. The cellular components in vascular neoplasms such as endotheliomas and angiosarcomas are composed of endothelial cells, which usually display a positive immunoreactivity against von Willebrand factor. The vessels in HEPs however, are lined by a single layer of von Willebrand factor-positive endothelial cells, while the perivascular tumour cells stain negative for von Willebrand factor (Enzinger and Weiss 1995; Gross et al. 2005; Baldi and Spugnini 2006; Avallone et al. 2007). To some extent, the heterogeneity in the histopathological and immunohistochemical appearance seen in neoplasms, which have conventionally been diagnosed as (C)HEPs, is believed to be attributable to the presence of different tumour entities originating from different cellular components of the subendothelial vascular wall (Avallone et al. 2007), commonly referred to as perivascular wall

tumours (including CHEPs, myopericytomas, angioleiomyomas/sarcomas, angiomyofibroblastomas and angiofibromas). In the present case, the lack of immunoreactivity against cytoplasmic contractile proteins helped to differentiate the diagnosis of a HEP from other perivascular wall tumours. The closest entity to consider in the differential diagnosis to HEP might finally be a glomus tumour, a rare neoplasm arising from the glomus body, a specialized form of arteriovenous anastomosis (Gross et al. 2005). The histological appearance of the two reported cases of a glomus tumour and a HEP in cats displays an extensive analogy to that of the respective "human" counterparts, characterized by perivascular proliferation of plump, neoplastic cells, and enmeshment of individual tumour cells by a well-developed network of thin argyrophilic fibrous material (Uchida et al. 2002; Gross et al. 2005; Baldi and Spugnini 2006). Although pericytes and glomus cells both share a common perivascular anatomical localisation, evidence exists that glomus cells are more closely related to smooth muscle cells than to pericytes (Weiss and Goldblum 2001). Correspondingly, human and feline glomus tumors display a positive immunoreactivity against markers of smooth musculature (Uchida et al. 2002; Gross et al. 2005), which was notably absent in the present case. As a further differential criterion, glomus tumours and HEPs generally tend to differ in their malignancy. Glomus tumours usually have a rather benign behaviour with non-infiltrative growth, formation of a collagenous capsule, and low tendencies towards recurrence (Uchida et al. 2002; Gross et al. 2005). In contrast, the malignant behaviour of the neoplasm in the present case was confirmed by its tendency to infiltrate the adjacent muscular tissue, the presence of necrosis, and the high number of mitotic figures. In summary, the present case adds to the previously reported occurrence of HEPs in cats. The pathological features of the documented cases of feline HEPs, including the present record, paralleled more closely the human HEP rather than the HEP found in dogs. However, due to the negligibly small incidence of this neoplasm in cats, an estimation of its potential morphological variability, malignancy and prognostic validation is not feasible. To obtain further insights into these areas, cases of HEP in cats should be thoroughly investigated and documented. As proposed in humans and dogs, the diagnosis of HEP in cats should be performed by careful exclusion of differential diagnoses, using an adequate spectrum of histological stains and immunohistological markers.

Acknowledgement

We thank Elisabeth Kemper, Heike Sperling, Michaela Nützel, Doris Merl and Angela Siebert for excellent technical assistance. This research received no specific grant from any funding agency in the public, commercial, or not-for-profit sectors. The authors do not have any potential conflicts of interest to declare.

REFERENCES

Avallone G, Helmbold P, Caniatti M, Stefanello D, Nayak RC, Roccabianca P (2007): The spectrum of canine cutaneous perivascular wall tumors: morphologic, phenotypic and clinical characterization. Veterinary Pathology 44, 607–620.

Baldi A, Spugnini EP (2006): Thoracic haemangiopericytoma in a cat. Veterinary Record 159, 598–600.

Chijiwa K, Uchida K, Tateyama S (2004): Immunohistochemical evaluation of canine peripheral nerve sheath tumors and other soft tissue sarcomas. Veterinary Pathology 41, 307–318.

Enzinger FM, Weiss SW (1995): Perivascular tumors. In: Enzinger FM, Weiss SW (eds.): Soft Tissue Tumors. 3rd ed. Mosby, St. Louis. 701–733.

Fletcher CDM, Unni KK, Mertens F (eds.) (2002): Pathology and genetics of tumours of soft tissue and bone. In: Kleihues P, Sobin LH (eds.): WHO Classification of Tumours. IARC Press, Lyon. 86–90.

Goldschmidt MH, Hendrick MJ (2002): Tumors of the skin and soft tissues. In: Meuten DJ (ed.): Tumors in Domestic Animals. 4th ed. Iowa State Press, Ames. 45–117.

Gross TL, Ihrke PJ, Walder EJ, Affolter VK (2005): Perivascular tumors. In: Gross TL, Ihrke PJ, Walder EJ, Affolter VK (eds.): Skin Diseases of the Dog and Cat. Clinical and Histopathologic Diagnosis. 2nd ed. Blackwell Science, Oxford. 759–765.

Handharyani E, Ochiai K, Kadosawa T, Kimura T, Umemura T (1999): Canine hemangiopericytoma: an evaluation of metastatic potential. Journal of Veterinary Diagnostic Investigation 11, 474–478.

Henderson DW, Papadimitriou JM, Coleman M (1986): Vasoformative tumours. In: Henderson DW, Papadimitriou JM, Coleman M (eds.): Ultrastructural Appearances of Tumours. Diagnosis and Classification of

Human Neoplasia by Electron Microscopy, 2nd ed. Churchill Livingstone, London. 247–253.

Hendrick MJ, Mahaffey A, Moore F, Vos J, Walder E (1998): Histological classification of the mesenchymal tumors of skin and soft tissues of domestic animals. In: WHO International Histological Classification of Tumors of Domestic Animals. 2nd Series. Armed Forces Institute of Pathology, Washington. 64 pp.

Hermanns W, Liebig K, Schulz LC (1981): Postembedding immunohistochemical demonstration of antigen in experimental polyarthritis using plastic embedded whole joints. Histochemistry 73, 439–446.

Mazzei M, Millanta F, Citi S, Lorenzi D, Poli A (2002): Haemangiopericytoma: histological spectrum, immunohistochemical characterization and prognosis. Veterinary Dermatology 13, 15–21.

Mulligan RM (1995): Hemangiopericytoma in the dog. American Journal of Pathology 31, 773–789.

Sawamoto O, Yamate J, Kuwamura M, Hagiwara R, Kurisu K (1999): A canine peripheral nerve sheath tumor including peripheral nerve fibers. Journal of Veterinary Medical Science 61, 1335–1338.

Schulman FY, Johnson TO, Facemire PR, Fanburg-Smith JC (2009): Feline peripheral nerve sheath tumors: histologic, immunohistochemical, and clinicopathologic correlation (59 tumors in 53 cats). Veterinary Pathology 46, 1166–1180.

Uchida K, Yamaguchi R, Tateyama S (2002): Glomus tumor in the digit of a cat. Veterinary Pathology 39, 590–592.

Weiss SW, Goldblum JR (2001): Perivascular tumors. In: Enzinger FM, Weiss SW (eds.): Soft Tissue Tumors. 4th ed. Mosby, St. Louis. 985–1001.

Xu FN (1986): Ultrastructure of canine hemangiopericytoma. Veterinary Pathology 23, 643–645.

Received: 2012–05–08
Accepted after corrections: 2012–05–14

Corresponding Author:

Dr. Andreas Blutke, Ludwig-Maximilians-Universitaet München, Institute of Veterinary Pathology at the Centre for Clinical Veterinary Medicine, Veterinärstr. 13, 80539 Munich, Germany
Tel. +49 89 2180 2590, E-mail: blutke@patho.vetmed.uni-muenchen.de